

Validation of the Estimated Torques of an Open-chain Kinematic Model of the Human Body

Bálint Petró¹, Rita M. Kiss^{1*}

¹ Department of Mechatronics, Optics and Mechanical Engineering Informatics, Faculty of Mechanical Engineering, Budapest University of Technology and Economics, Műgyetem rkp. 3., H-1111 Budapest, Hungary

* Corresponding author, e-mail: rita.kiss@mogi.bme.hu

Received: 27 January 2022, Accepted: 11 March 2022, Published online: 21 March 2022

Abstract

The standing human body is frequently modeled as an inverted double pendulum restricted to a single plane. In order to capture the coordination efforts and interplay between spatial dimensions, the model has to capture motion and joint torques in all spatial dimensions. Our two-segment model covers two degrees of freedom (ML and AP revolutions) at the ankle and the hip level and utilizes the Denavit-Hartenberg convention. This work aimed to validate the model's torque estimation on a diverse group of participants (11 women, 22–56 years, 11 men, 22–61 years). The inverse dynamic calculations provide estimated joint torques for a motion capture recorded trial, while standing on a force platform enables the indirect measurement of ankle torques. A 60-second-long visually guided balancing task was recorded and repeated three times. The estimated and the indirectly measured torques were compared, and offset and variance type errors (normalized RMSE and R^2) were analyzed. The R^2 -values were excellent ($R^2 > 0.90$) 64 out of the 66 cases (97%) for AP torques and 58 out of the 66 cases (88%) for ML torques. Normalized RMSE values were dominantly under the 0.35 value with some outliers. RMSE showed no evident connection with age, body height, body mass, or BMI. An open-chain kinematic model with two segments, following the Denavit-Hartenberg convention, is well suited to estimate the control torque traces of the human body during standing balancing and needs only three tracked positions.

Keywords

inverse dynamics, open-chain model, joint torque, balancing

1 Introduction

Numerous biomechanical models have been developed to describe the motion of the human body [1]. It is well established in the literature that balancing involves several common coordination strategies in order to reduce the degrees of freedom and achieve fast enough responses. In standing balance, the ankle-hip strategy approach distinguishes three strategies, i.e., the ankle-dominant, the hip-dominant, and the ankle-hip mixed strategies [2]. The ankle strategy primarily appears for anterior-posterior (AP) tasks; muscles of the ankle and the shank start activation, and the entire body rotates around the ankle's axis approximately as a single rigid link [3, 4]. The hip strategy primarily coordinates the body into two relatively rigid links, i.e., the lower and upper bodies. One segment produces leans in one direction, and the other segment a countermovement by leaning in the opposite direction. The hip strategy is dominant in medio-lateral (ML) tasks [5], especially in shifting the COM in the ML direction; however, the hip is also used in large-amplitude AP tasks.

The applied biomechanical model is chosen regarding the motion strategies that are to be detected. Inverted double pendulum models are frequently employed to detect the presence of the ankle or the hip strategy. The dominant joint is determined by the modeled joint angles (the angles between the modeled rigid body links) and the changes of these angles. Notably, most biomechanical models are restricted to a single plane (either AP or ML) [1], which may seem to be an economical choice that considers the motion constraints of the balancing tasks or devices being used [6]. However, this is a limitation as it removes the possibility to analyze any interplay between the different spatial dimensions.

It is feasible that the human body might naturally use all available directions, especially near the limits of stability or in the case of difficult balancing tasks. In their seminal work, Hof et al. [7] stated that simply projecting the COM vertically to the ground and comparing that to the base of

support (BOS) limits to determine stability may be sufficient for static stability; this distance is further reduced by a term arising from the velocity towards the limit. It follows that as the COP moves closer to the limit of stability (the limit of the base of support), the nervous system may instinctively try to increase the margin of stability by way of not only reducing but redirecting the vector of the momentum of the COM away from the limit. Following a sudden lateral perturbation while standing on a freely oscillating platform, we had frequently noted such interplay when significant motion in the AP plane appeared to either improve the chances of successful balance recovery or enhance the effectiveness of the action [8].

In order to capture the coordination efforts and interplay between spatial dimensions, a biomechanical model is needed that is capable of capturing the motion in all spatial dimensions and also the joint torques that arise to execute such maneuvers. We have earlier utilized an open-chain kinematic model (Fig. 1) constructed according to the Denavit-Hartenberg (D-H) convention to analyze the body's motion following a perturbation test on a freely oscillating platform [9]. The foundational premise of the

D-H convention is that by assigning reference frames to each of the rigid body links accordingly to the convention, it is possible to describe the pose, i.e., the links' location and orientation using only four parameters. The advantages of the D-H convention arise from the ease of formulation and the straightforward derivation of the equations of motion as this process can be done algorithmically. In addition, the model yields joint angles and torques that are readily interpretable from a biomechanical perspective.

The aim of the present study was to validate the estimated torque values and signals obtained from the two-link D-H model via validation measurements on an inhomogeneous group of healthy adult participants. The validation's basic premise was to compare the indirectly measured torques with the model estimated torques arising at the ankle level during a visually guided balancing task to obtain standard, repeatable balancing motion while standing on a force-measuring platform.

2 Methods

2.1 The double-pendulum model

The applied model was constructed using the D-H convention modified by Khalil and Dombre [10]. The model is a double-pendulum model, consisting of a lower-body link (covering the shanks and thighs) and an upper-body link (covering the pelvis, trunk, arms, neck, and head) with four single rotational degree-of-freedom joints (Fig. 1). The D-H parameters are given in Table 1.

The arms were modeled as mass points; left and right shanks and thighs as two touching cylinders each; trunk-pelvis and neck-head as one cylinder each. Weight, inertia, and center of mass values were calculated for body segments (shank, thigh, lower-, upper-, middle-trunk, head, upper arm, lower arm) based on proportional values [11] of total body mass and height. The respective body segments for the two DP links were then summed up to obtain the link's final inertial properties in question. Specifically, the first (lower) link constitutes the feet, the shanks, the thighs, and the lower trunk; the second (upper) link constitutes the middle-trunk, the upper-trunk, the head, the upper arms, and the lower arms.

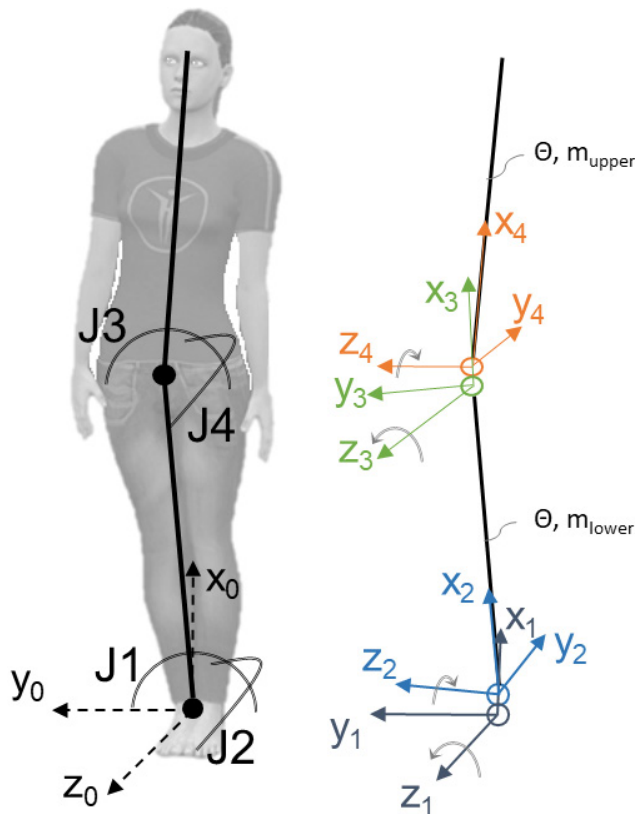


Fig. 1 Double pendulum model for the balancing human body. The first reference frame in its initial position coincides with the global reference.

Table 1 D-H parameters of the model

| joint | α_i | θ_i | a_i | d_i |
|-------|------------|------------|-----------|-------|
| J1 | 0 | Q_1 | 0 | 0 |
| J2 | $-\pi/2$ | Q_2 | 0 | 0 |
| J3 | $\pi/2$ | Q_3 | L_{leg} | 0 |
| J4 | $-\pi/2$ | Q_4 | 0 | 0 |

The first two joints allow lateral (Joint1) and frontal (Joint2) rotation at the ankle level; the second two joints allow lateral (Joint3) and frontal (Joint4) rotation at the hip level. Tracking only three spatial points (the midpoint of the ankle joints, the hip joints, and the head) gives enough information to calculate the positions and orientations of the model. Joint angles are easily obtained via trigonometric calculations, and second-order Lagrange functions give the equations of motion, producing the joint torques for each recording timeframe.

A key issue is the simplification at the ankle joint level. It is assumed that in the modeled position (upright standing), the actual ankle joints will be close to each other and thus rotate together. Consequently, the ankle joint is modeled in the midway point of the actual ankles as a single point with a static position relative to the ground reference. At the same time, this implies that the rotational axis will stay at the midway point of these. However, sideways rotation of the lower body is induced by two mechanisms, i.e., the invertor/evertor torques from the ankle muscles and the load/unload mechanism from the load shift between the two feet. If the load shifts from the center towards one of the ankles, this may lead to a ML shift in the position of the rotational axis itself.

2.2 Participants, measurements, and protocol

In accordance with the goal of this investigation, an inhomogeneous participant group was recruited. Eleven women (22–52 years) and 11 men (22–61 years) participated (Table 2). Exclusion criteria were vision correction greater than ±5.0 diopters, musculoskeletal alterations, or the presence of muscle or joint pain.

Table 2 Anthropometric data for the participant group

| | | women | | | men | | | |
|-----|-----------------|----------------|-----|-----|-----------------|----------------|-----|--|
| age | body height (m) | body mass (kg) | BMI | age | body height (m) | body mass (kg) | BMI | |
| 22 | 1.56 | 71 | 29 | 22 | 1.83 | 132 | 39 | |
| 23 | 1.67 | 79 | 28 | 26 | 1.83 | 78 | 23 | |
| 24 | 1.77 | 63 | 20 | 27 | 1.82 | 80 | 24 | |
| 24 | 1.69 | 63 | 22 | 27 | 1.76 | 88 | 28 | |
| 25 | 1.68 | 60 | 21 | 28 | 1.96 | 76 | 20 | |
| 32 | 1.83 | 63 | 19 | 31 | 1.92 | 89 | 24 | |
| 36 | 1.72 | 62 | 21 | 34 | 1.77 | 82 | 26 | |
| 37 | 1.81 | 67 | 20 | 42 | 1.78 | 114 | 36 | |
| 40 | 1.74 | 66 | 22 | 46 | 1.73 | 56 | 19 | |
| 48 | 1.69 | 76 | 27 | 59 | 1.88 | 92 | 26 | |
| 52 | 1.62 | 75 | 29 | 61 | 1.69 | 73 | 26 | |

To fully describe the body's movement in the spatial domain, only three points have to be tracked, as shown in Fig. 2, i.e., a point at the ankle, at the hip, and at the head.

To achieve this, the participants were equipped with three retro-reflective marker clusters that were tracked by an 18 infra-red camera motion capture system (OptiTrack, NaturalPoint Inc., Oregon, USA) at a sampling rate of 100 Hz. This system has a sub-millimeter accuracy [12], while the expected movements to be recorded for the balancing tasks are in the order of centimeters. Marker clusters were placed on the lower right shank, above the sacrum, and on the head, applied with a strap (Fig. 2). The tracked marker clusters' pivot point was calibrated manually to the estimated joint axis midpoints for each participant. The lower joint position was set to where the

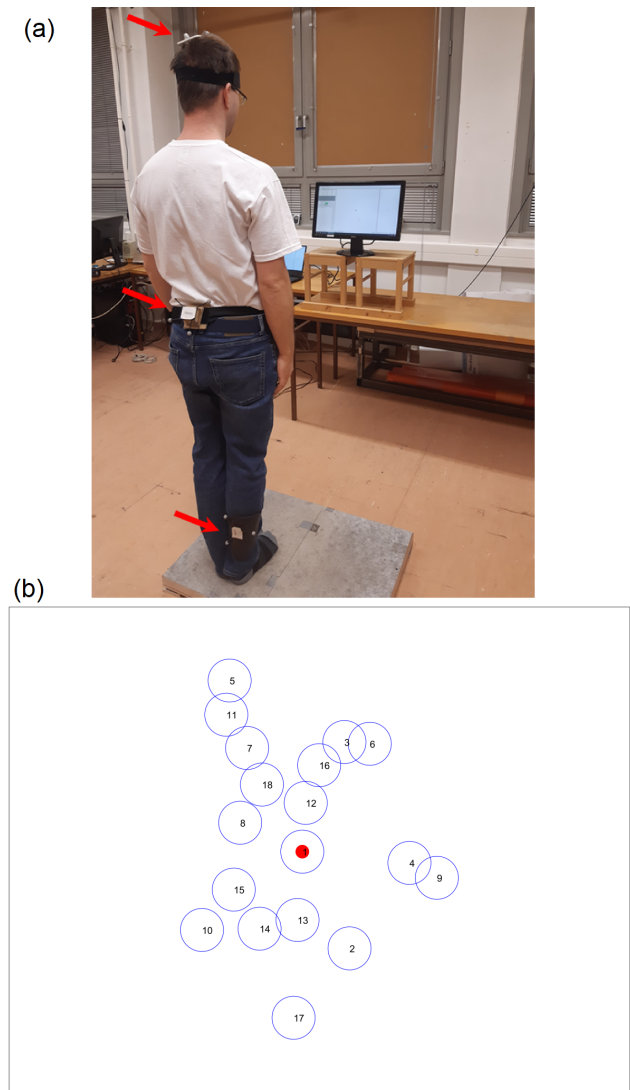


Fig. 2 (a) Measurement setup (arrows indicate marker clusters); (b) visual balancing task. The targets are shown here together; numbers indicate the order of appearance

ankles touched each other, or in the case of genu valgus, to the midpoint between the two medial malleoli. There was only a technical reason for setting the shank marker cluster's pivot point as the ankle joint position, i.e., the visual feedback system required streamed, real-time data. However, during preprocessing, the ankle positions were set to the average measured position as a static value since participants were instructed not to move their feet during the measurement. The middle joint position point was set as the sacrum marker cluster's pivot point, specifically to the midpoint between two calibration markers placed on the trochanter majors. The upper tracked point was set to the apex of the head, in the plane of the ears, in the middle.

The motion capture system broadcasted the tracked pivot points as joint positions to a custom-made visual software for the visual balancing task. The same anthropometric proportional data [11] used for the double-pendulum model was applied here to estimate the COM of the lower- and upper bodies, which were then summed up proportionally. The estimated full-body COM-position in the horizontal plane was then visualized as a cursor to be moved (Fig. 2). The cursor's position was offset to the middle after asking the participant to assume a normal, comfortable upright position.

Ground reaction forces were measured by a single P6000-type force platform (BTS Bioengineering S.p.A., Italy). The platform can measure reaction forces in all three spatial dimensions with a precision of 1 N. The sampling frequency was set to 1 kHz. Participants stood in the middle of the platform, wearing only socks.

The protocol for the motion recordings was as follows. After applying the marker clusters and calibrating the joint positions (done by the same examiner), the participants were asked to stand in the middle of the force platform, ankles and toes touching, arms kept at their sides, approximately 1.2 m away from a computer display (Fig. 2 (a)). Participants were then presented with the visual balancing task to familiarize themselves with the program. Their COM was displayed without noticeable delay as a red dot on the screen (Fig. 2 (b)). The dot moves up and down as the COM is moved forward and backward, respectively, and left to right with sideways COM motions. They were instructed that blue circles (targets) would appear, one at a time, and their task was to reach the middle of each target circle as fast as possible and stay within the circle afterward. They were not allowed to move their feet during a trial, and arms had to be kept in contact with their sides. Each circle was displayed for 3.5 s, after which a new one

appeared. The circles' sequence was generated randomly beforehand and fixed during the measurements for all participants and trials. The first target circle was centered on the initial position. One sequence lasted 60 s, after which a 60 s break was included when the participant had to step off the platform and move about the room. The task was repeated three times.

2.3 Data processing

After exporting the motion capture and the force platform data, all post-processing was performed in a custom Matlab (version R2018b) script. The force platform data were decimated to match the measurement frequency of the motion data. The indirectly *measured ankle torques* (T) were calculated as the cross-product of the ground reaction force vector and the moment arm between the force vector's point of attack and the ankle joint axis point. Consequently, if the ankle's measured position, calibrated to the midway point of the two ankles, has a static position error, that would cause a static, offset-type error in the measured torque.

In order to minimize the calibration position errors, it was first assumed that in the initial, normal upright stance the loadings of the feet would be equal, meaning zero ML ankle and hip angles and torques. Based on this assumption, the ML positions of the tracked points (ankle, hip, and head) were offset in the ML direction with the mean value of the first two seconds of the recording. It was also assumed that the COP would be anterior to the ankle axis in the initial stance, as normally a plantarflexion torque at ankle level maintains balance against the toppling torque. For this reason, we could not use an offset step for the AP positions.

To obtain the *model-estimated ankle torques*, the offset joint positions were first converted into joint angle values (Q) using trigonometric functions, which were then smoothed, and angular velocities and accelerations were obtained by numerical derivation. Then, the double-pendulum model's equations of motion were applied for each time frame to obtain the estimated joint torques for all four modeled joints.

To validate the model, we compared the time traces of the measured and modeled torques, and we calculated the error torque, specifically considering errors in values and errors in signal shape. As quantitative error metrics, we calculated the (RMSE) (root mean square error) normalized by the interquartile range to determine the goodness of fit in absolute values and the R^2 (coefficient of

regression) to determine the goodness of fit for the signals' shape. The offset error was calculated for the ankle AP torques as the mean difference between torques (estimated minus measured) for the first two seconds to quantify the calibration error. RMSE for ankle AP torque was calculated after zero-mean offsetting the signals to mitigate the effects of position calibration errors on this metric. Finally, we analyzed the effects of different body types by comparing the correlation between the error metric results and the anthropometric data.

3 Results

The 22 participants together successfully produced 66 motion records. An example of the measured and calculated joint angles and torques is shown in Fig. 3. Visual inspection showed an excellent match for the shape of the torque traces. The shape of the error torque trace showed that the error is primarily noise with zero mean (Fig. 3). A possible source of the peaks and the shape of the error may be the small time shifts in the two traces due to numerical errors and shifts caused by filtering. This enhances the errors where the rate of change in torque values is high. However, the signal characteristics remained well-preserved.

For the group, the AP ankle torque offset error had a median of 9.48 Nm with an interquartile range of [4.73 Nm, 16.71 Nm], which corresponds to percentage values of 23.33% median with an interquartile range of [11.62%, 51.95%]. This means that the estimated AP ankle torque was typically greater than the measured one. The R^2 -values were excellent ($R^2 > 0.90$) for 64 out of the 66 cases (97%) for AP torques and for 58 out of the 66 cases (88%) for ML torques (Fig. 4). Normalized RMSE values were dominantly under the 0.35 value with few outliers (4) and were slightly greater in the ML direction.

Comparing normalized RMSE with anthropometric measures (Fig. 5), the error metric showed no evident connection with age, body height, body mass, or BMI.

4 Discussion

This investigation aimed to compare the model-estimated and the indirectly measured torques for an anthropometrically diverse group of participants. We obtained the model-estimated torques from the motion capture data via inverse dynamics calculations, while the indirectly measured torques were obtained from a simple calculation using the force platform and the ankle axis position data.

The match in signal shape was excellent in both directions, supported by the high R^2 values. As such, it can be stated that the model estimated the torque traces superbly. However, an offset-type error was present, which was substantial in some cases.

The possible offset errors arose from the inaccurate calibration of the rotational axis, i.e., the joint mid-point, since this adds a constant offset to the joint angle values. This was successfully mitigated for the ML torques via offsetting the ML positions of the tracked points. However, this was not viable for the AP direction, since the natural standing posture involves a slight forward tilt, which should be preserved in the model. The offset errors caused the AP ankle torque to typically be 11.6%–51.95% greater than the measured torque, which is a substantial amount. A possible approach to minimize calibration errors is to track multiple points around the joint of interest and then calculate a weighted sum of these to estimate the mid-point. However, modifying the measurement setup this way may not be viable. Considering this, an approach may be taken where the joint torques are decomposed into a static, passive component and an active control torque. Then, the estimated ML and AP control torques would be correct in shape and close to the actual values as well.

Regarding the practical utility of the results, the D-H model yields torques that are biomechanically readily interpretable. Furthermore, the model can be easily extended to include more segments in the open chain, e.g., to include the knee as a single degree of freedom joint, or to consider multiple segments in the torso. A clinical application would be a simple measurement setup where a limited number of points are tracked on the patient's body, and the model calculated the controlling torques in the modeled joints in an effort to better quantify the results of standing balancing tests. In particular, the method detects the dominance of joints, the applied balancing strategy, and the co-ordinational efforts between the spatial dimensions, as demonstrated in [9].

A limitation of this investigation is that only a single force platform was used to measure ground reaction forces. Further measurements using two force platforms, standing with one foot on each, would offer the benefit of capturing the shifting load between the feet that could help in determining how this influences the rotational axis. An additional hurdle in the validation process is that while the model estimates torques for all joints, which is a major advantage, the hip torques cannot be validated

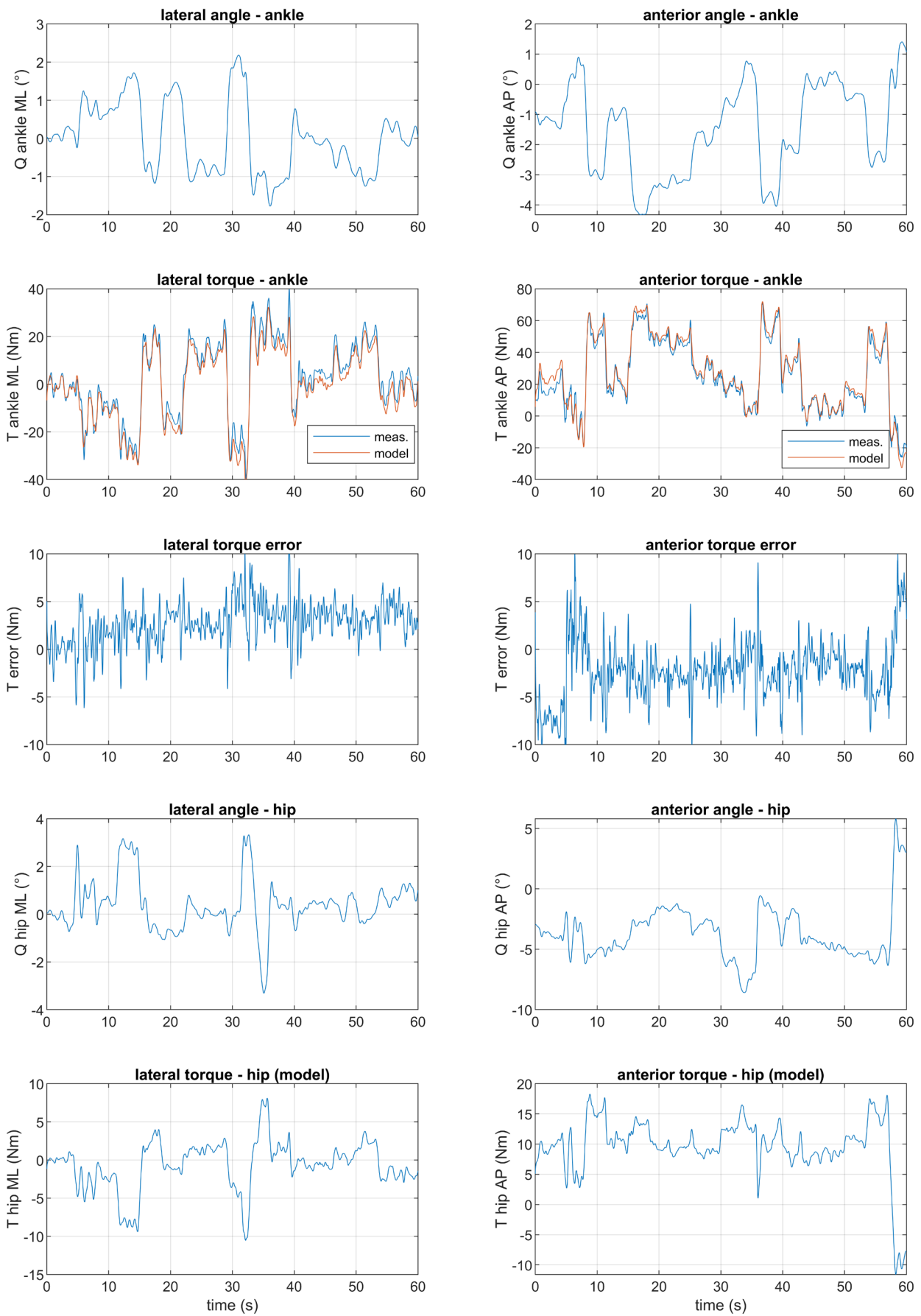


Fig. 3 Example of estimated and measured torques and the error traces

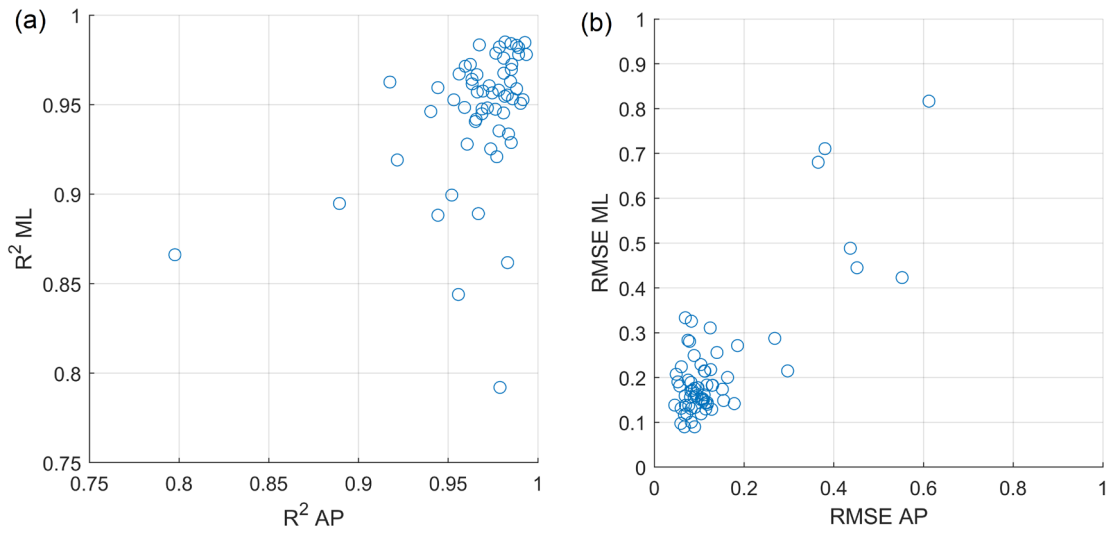


Fig. 4 Error metrics of torque estimation: (a) R^2 ; (b) RMSE

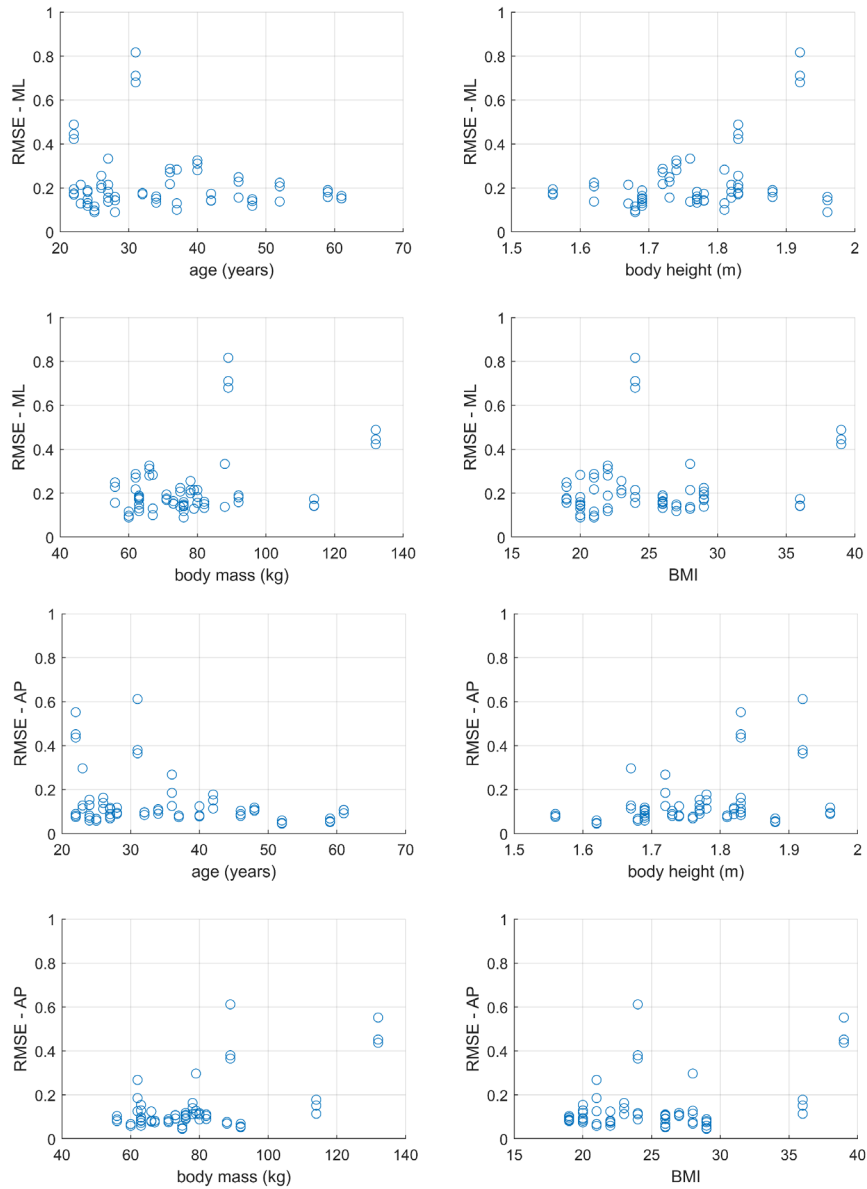


Fig. 5 Correlation of RMSE with anthropometric data

via measurements. In addition to the time domain analysis, a frequency domain comparison would be beneficial in the case of shorter recordings to see if both the slower, large amplitude, and faster, small amplitude components are well preserved.

5 Conclusion

In summary, we carried out validation measurements for an open-chain kinematic model with two segments. The indirectly measured ankle torques were compared with the model estimated torques arising at the ankle level during a standing balancing task on an inhomogeneous group of healthy adult participants. The model showed to be well-suited to estimate the torque traces for a wide range of body types. The match in torque values was excellent for both ML and AP torques, with a static (offset) error in AP torque due to a calibration error of the joint position. Utilizing the model is a simple way of

estimating the control torques to characterize the balancing motion, the dominance of a hip or ankle strategy, and the coordination between the spatial dimensions. Further measurements are needed with multiple force platforms to investigate the effects of load shifting and measuring the knee position to allow for a triple-segmented model to be formulated.

Acknowledgement

The authors thank Ambrus Zelei, Ph.D. for helpful discussions regarding the open-chain kinematic models.

The research reported in this paper is part of project no. BME-NVA-02, implemented with the support provided by the Ministry of Innovation and Technology of Hungary from the National Research, Development and Innovation Fund, financed under the TKP2021 funding scheme and by the Hungarian Scientific Research Fund, grant number OTKA K135042.

References

- [1] Créteil, A. "Which biomechanical models are currently used in standing posture analysis?", *Neurophysiologie Clinique/Clinical Neurophysiology*, 45(4–5), pp. 285–295, 2015.
<https://doi.org/10.1016/j.neucli.2015.07.004>
- [2] Horak, F. B., Nashner, L. M. "Central Programming of Postural Movements: Adaptation to Altered Support-Surface Configurations", *Journal of Neurophysiology*, 55(6), pp. 1369–1381, 1986.
<https://doi.org/10.1152/jn.1986.55.6.1369>
- [3] Almeida, G. L., Carvalho, R. L., Talis, V. L. "Postural strategy to keep balance on the seesaw", *Gait & Posture*, 23(1), pp. 17–21, 2006.
<https://doi.org/10.1016/j.gaitpost.2004.11.020>
- [4] Chagdes, J. R., Rietdyk, S., Haddad, J. M., Zelaznik, H. N., Raman, A. "Dynamic stability of a human standing on a balance board", *Journal of Biomechanics*, 46(15), pp. 2593–2602, 2013.
<https://doi.org/10.1016/j.jbiomech.2013.08.012>
- [5] Orrell, A. J., Eves, F. F., Masters, R. S. W. "Implicit motor learning of a balancing task", *Gait & Posture*, 23(1), pp. 9–16, 2006.
<https://doi.org/10.1016/j.gaitpost.2004.11.010>
- [6] Petró, B., Papachatzopoulou, A., Kiss, R. M. "Devices and tasks involved in the objective assessment of standing dynamic balancing – A systematic literature review", *Plos One*, 12(9), Article ID: e0185188, 2017.
<https://doi.org/10.1371/journal.pone.0185188>
- [7] Hof, A. L., Gazendam, M. G. J., Sinke, W. E. "The condition for dynamic stability", *Journal of Biomechanics*, 38(1), pp. 1–8, 2005.
<https://doi.org/10.1016/j.jbiomech.2004.03.025>
- [8] Petró, B., T Nagy, J., Kiss, R. M. "Effectiveness and recovery action of a perturbation balance test – a comparison of single-leg and bipedal stances", *Computer Methods in Biomechanics and Biomedical Engineering*, 21(10), pp. 593–600, 2018.
<https://doi.org/10.1080/10255842.2018.1502278>
- [9] Petró, B., Kiss, B., Kiss, R. M. "Analyzing human balance recovery action using calculated torques of a double pendulum model", *Materials Today: Proceedings*, 12(2), pp. 431–439, 2019.
<https://doi.org/10.1016/j.matpr.2019.03.146>
- [10] Khalil, W., Dombre, E. "Modeling, Identification and Control of Robots", Taylor & Francis, New York, NY, USA, 2002.
- [11] de Leva, P. "Adjustments to Zatsiorsky-Seluyanov's segment inertia parameters", *Journal of Biomechanics*, 29(9), pp. 1223–1230, 1996.
[https://doi.org/10.1016/0021-9290\(95\)00178-6](https://doi.org/10.1016/0021-9290(95)00178-6)
- [12] Nagymáté, G., Tuchband, T., Kiss, R. M. "A novel validation and calibration method for motion capture systems based on micro-triangulation", *Journal of Biomechanics*, 74, pp. 16–22, 2018.
<https://doi.org/10.1016/j.jbiomech.2018.04.009>